International Journal of Engineering Research-Online
A Peer Reviewed International Journal
Articles available online http://www.ijoer.in

Vol.3., Issue.6., 2015
(Nov.-Dec.,)

RESEARCH ARTICLE

ISSN: 2321-7758

CONTROL OF TWO-PHASE INDUCTION AND SYNCHRONOUS MOTOR DRIVES USING DIRECT TORQUE CONTROL

D.SREEKANTHREDDY

M.TECH, POWER ELECTRONICS AND DRIVES (2ND YEAR)
VIT UNIVERSITY

D.SREEKANTHREDDY

ABSTRACT

Single phase induction motors are widely used in household products and low-power industrial equipments. As the centrifugal switch doesn't disconnect the auxiliary winding in low speed operation, single phase induction motors operation in wide speed range is practically inaccessible. So, in variable speed application, torque ripple and over temperature are problematic. These can be overcome by utilizing three-leg inverter and using both motor windings. But the difficulty in this method is that the auxiliary winding voltage should be higher than that of main winding. So using boost converters or placing a capacitor in series with the auxiliary winding, is required for high-speed (e.g. rated speed) applications. Because of the cost attributed to these approaches, speed control of symmetrical two-phase induction motors is preferred. When good performance of motor drive is expected, utilizing high performance control methods is inevitable. Vector control of symmetrical two-phase induction motor is proposed as a solution for low-power level field; but suggested scheme needs utilization of mechanical sensors which makes the drive system costly. On the contrary, good performance of DTC method without using speed or position sensors makes it a viable choice in both high performance and low-cost applications. In this paper the simulation of DTC of two phase motors is carried out by using MATLAB/SIMULINK and the results are analysed.

Key words: two phase induction and synchronous motors, direct torque control(DTC),inverters.

I. INTRODUCTION

In 1977,Emotron was the first company to introduce an AC drive based on pulse width modulation (PWM).Further developments led to one of the first market launches of AC drives with direct torque control in 1998.TheEmotron technology has an extremely first response time since actual and required torque is compared 40,000 times a second. Because of some features such as low cost and simple and robust structure, single phase induction motors are widely used in household products and low-power industrial equipments. Single phase induction motor is an asymmetrical two-phase induction motor including the main can dc the auxiliary windings. Three common types of single phase induction motors are split-phase, capacitor-

start and capacitor-run motors . Single phase motors work well in constant-speed applications, but show difficulties when variable-speed performance is needed. In both-split-phase and capacitor-start single phase motors, operation in wide speed range is practically inaccessible because in low speed operation, the centrifugal switch doesn't disconnect the auxiliary winding. This causes damages to the motor structure since the auxiliary winding is not designed for continuous operation. In capacitor-run motors, the appropriate capacitance depends on the conditions of power supply and mechanical load. So, in variable speed application, torque ripple and over temperature are problematic .It's possible to overcome the stated problems by utilizing three-leg inverter and using both motor windings. Difficulty of this method is that the auxiliary winding voltage should be higher than that of main winding, so using boost converters or placing a capacitor in series with the auxiliary winding is required for high-speed (e.g. rated speed) applications .It's possible to overcome the stated problems by utilizing three-leg inverter and using both motor windings. Difficulty of this method is that the auxiliary winding voltage should be higher than that of the main winding so using boost converters or placing a capacitor in series with the auxiliary winding is required for high-speed (e.g. rated speed) applications . Because of the cost attributed to these approaches, speed control of symmetrical two-phase induction motors is preferred. Another alternative is utilization of two-phase synchronous drives which introduces higher torque density and thus more compact size. Common structures of two phase inverters shown in Fig.1 have been studied . The operation of two-leg inverter shown in Fig.1.a is weak, but because of possessing minimum number of switches, it is a low-cost approach. Inthe applications in which the middle-point of DC voltage is accessible, using two-leg inverter is an acceptable approach When middle-point of DC voltage is inaccessible, utilizing this scheme needs not only two capacitors with high capacitances but also a voltage equalizing circuit. Voltage equalization can be done by using resistors in parallel to capacitors. This increases volume of the drive system and power loss .Another approach is utilization of charge balancing circuits which makes the drive circuit complicated and costly. A noticeable limitation of three-leg inverters in controlling two-phase motors is that the RMS value of common leg current is higher than those of other two legs that necessitates utilization of switches with higher current ratings at least in one leg. When integrated power modules (IPMs) are used, the entire module should be of higher current ratings. This makes the cost enhancement more noticeable. This additional cost as well as better performance of four-leg inverter makes the use of four-leg inverter justifiable in high performance applications .When good performance of motor drive is expected, utilizing high performance control methods is in evitable .Vector control of symmetrical two-phase induction motor is proposed in as a solution for low-power level field; but suggested scheme needs utilization of mechanical sensors which makes the drive system costly. On the contrary, good performance of DTC method without using speed or position sensors makes it a viable choice in both high performance and low-cost applications.

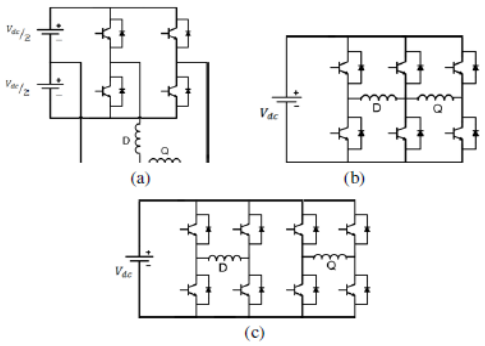

Figure1.Different inverter topologies used in two-phase motor drives (a) two-leg inverter (b)three-leginverter(c)four-leginverter

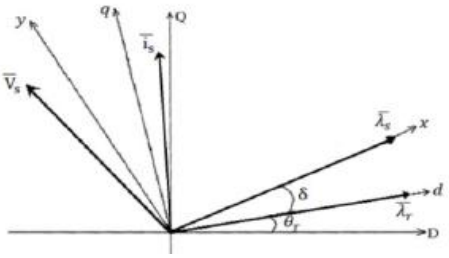

Figure2.stator and rotor flux vectors in deferent reference frames

Direct torque control of two-phase induction motors using two- and three-leg inverters has been studied in the literature. In both inverter topologies, in some regions of stator flux, the torque control fails. In high speeds, the trouble gets worse. Changing the switching table for improving the torque control. Using this approach not only makes the control system complicated, but also discards flux control in some areas of stator flux. In high speed operation, utilizing modified switching table leads to losing flux control in a wide area and in efficient operation of control system .In this paper, because of prominent features of two-phase motors in variable speed applications, utilizing these motors is suggested instead of single phase induction motors. Main application of two-phase motor drives would be in low power industrial applications as well as in household products such as refrigerators, vacuum cleaners, fans, air conditioners, water pumps etc. Direct torque control as a low cost, high reliable and high performance control method for two-phase induction and synchronous motors is proposed and switching tables for two-, three- and four- leg inverter topologies are presented. Different inverter topologies are compared in terms of drive system ability to control electromagnetic torque and maximum speed of rotating field provided by the drive system. Performance of DTC of two phase induction and synchronous motors fed by different inverter topologies are evaluated and correctness of presented formulas is validated by experimental results.

Principle of direct torque control of induction motor:

Direct torque control was developed by Takahashi and Depenbrock as an alternative to field-oriented control. In a direct torque controlled (DTC) induction motor drive supplied by a voltage source inverter, it is possible to control directly the stator flux linkage *s* ψ (or the rotor flux *r* ψ or the magnetizing flux *m* ψ) and the electromagnetic torque by the selection of an optimum inverter voltage vector. The selection of the voltage vector of the voltage source inverter is made to restrict the flux and torque error within their respective flux and torque hysteresis bands and to obtain the fastest torque response and highest efficiency at every instant. DTC enables both quick torque response in the transient operation and reduction of the harmonic losses and acoustic noise. As it has been introduced in expression the electromagnetic torque in the three phase induction machines can be expressed as follows :

$$t_e = \frac{3}{2} P \bar{\Psi} \times \bar{i_s}$$

Where $\Psi_s$is the stator flux,$i_s$is the stator current (both fixed to the stationary reference framefixed to the stator) and P the number of pairs of poles. The previous equation can be modifiedand expressed as follows:

$$t_e = \frac{3}{2} P \overline{\Psi_s} \times \bar{i_s} \cdot \sin(\alpha_s - \rho_s)$$

Where$\rho_s$is the stator flux angle and $\alpha_s$is the stator current one, both referred to thehorizontal axis of the stationary frame fixed to the stator. If the stator flux modulus is keptconstant and the angle ρsis changed quickly, then the electromagnetic torque is directly controlled. The same conclusion can be obtained using another expression for the electromagnetic torque .From the above equation next equation can be written:

$$t_e = \frac{3}{2} P \frac{L_m}{L_s L_r - L_m^2} |\overline{\Psi_r}'| \times |\Psi_s| \cdot \sin(\rho_s - \rho_r)$$

Because of the rotor time constant is larger than the stator one, the rotor flux changes slowly compared to the stator flux; in fact, the rotor flux can be assumed constant. (The fact that the rotor flux can be assumed constant is true as long as the response

time of the control is muchfaster than the rotor time constant). As long as the stator flux modulus is kept constant, thenthe electromagnetic torque can be rapidly changed and controlled by means of changing the angle$\rho_s - \rho_r$.

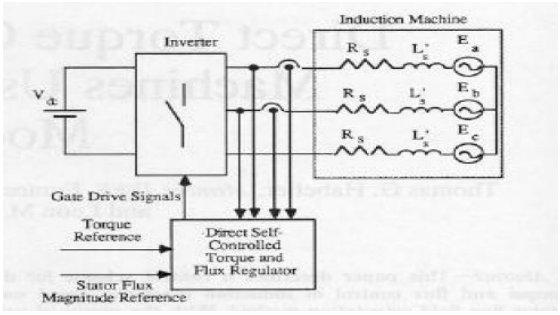

Figure3.Block schematic of direct torque control and flux controlled induction machine drive.

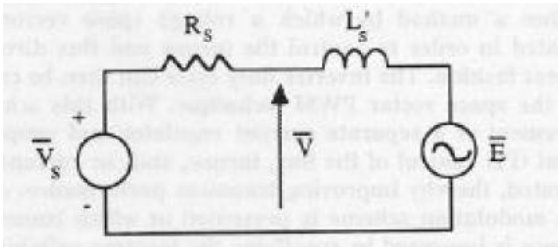

Figure4.Equivalent circuit of inverter driven induction machine in the dq stationary reference frame.

II.TWO PHASE INDUCTION MOTOR

The use of representative space phasors simplifies the mathematical model of the motors with cylindrical symmetry, as is the induction motor. The main advantage is that it facilitates the understanding of the phenomena occurring in the motor, through the direct link between the representative space phasor of the current and the magnetic voltage produced by a poly phased winding. These advantages are best illustrated within the "field control" of the induction motor. The structure of the indirect vector controlled two-phase induction motors, fed by an PI current controlled PWM voltage fed converter. The field orientation was made according to the rotor flux vector. To control position of two-phase induction motor with three phase inverter, the induction motor is connected as an unbalanced load between the three arms of the inverter. Control strategy seeks to maintain a constant 90° phase shift between currents in two phases and adjust the position. It is envisaged also maintain a certain torque irrespective of rotational speed of the induction motor .The two-phase induction motor is composed of two asymmetrical windings. Therefore, the auxiliary winding usually has fewer turns than the main winding and is displaced at ninety electrical degrees between these winding. Fig. 3 shows the schematic view of a two phase induction motor, illustrating that the auxiliary (α) windings and main (β) windings are not identical sinusoidal distributed windings, but are arranged space quadrature.

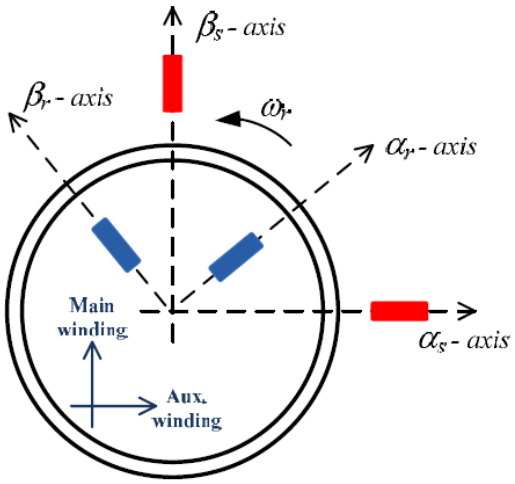

Figure5.asymmetrical two phase induction motor

III. DIRECT TORQUE CONTROL OF TWO-PHASE INDUCTION AND SYNCHRONOUS MOTORS

A. Basic Principles

For analyzing DTC method, first, equations of two-phase induction motor are studied. It's assumed that air gap length is constant and magnetic circuit is linear. Fig.2 shows the stator and rotor linkage flux vectors in rotor flux (d q), stator flux (x y), and stationary (DQ) reference frames. According to and by using voltage-current equations, stator fluxes of D and Q axes in stationary reference frame and electromagnetic torque of two-phase induction motor can be defined as:

$$\lambda_{Qs}=\int(\upsilon_{Qs} - r_s i_{Qs})dt \qquad (1)$$

$$\lambda_{Ds}=\int(\upsilon_{Ds}-r_s i_{Ds})dt \quad (2)$$

$$|\bar{\lambda_S}|=\sqrt{\lambda_{Qs}^2+\lambda_{Ds}^2} \quad (3)$$

T_e=P($\lambda_{Ds}i_{Ds}$-$\lambda_{Qs}i_{Ds}$) =p$\frac{L_m}{L_s'L_r'}\bar{\lambda_s}\times\overline{\lambda_r'}=P\frac{L_m}{L_s'L_m}\sin(\theta_s-\theta r$(4)

Where$r_s$is resistance of the stator winding;$\bar{\lambda_s}$, $\overline{\lambda_r'}$ Respectively are the stator flux vector and the rotor flux vector;υ_{Qs} ,υ_{Ds} ,i_{Qs} ,i_{Ds} ,$\lambda_{Qs}$and λ_{Ds}respectively are stator voltage components, stator current components and stator flux components in Q and D axes. Also, L_s , L_r' , L_m,and P respectively are stator inductance, rotor inductance referred to stator side, magnetizing inductance and number of motor pole pairs. In addition,θ_s ,$\theta_r$and δ are stator flux angle, rotor flux angle and load angle, respectively and

$$L_s'=(1-\frac{L_m^2}{L_sL_r'})L_s \quad (5)$$

A similar analysis is performed to study the DTC method of synchronous motor. Regarding and, using voltage-current equations of the motor, stator flux components in stationary reference frame and Electromagnetic torque of two-phase synchronous motor can be calculated as:

$$\lambda_{Qs}=\int(\upsilon_{Qs}-r_s i_{Qs})dt+\lambda_{Qs}|_{t=0} \quad (6)$$

$$\lambda_{Ds}=\int(\upsilon_{Ds}-r_s i_{Ds})dt+\lambda_{Ds}|_{t=0} \quad (7)$$

$$|\bar{\lambda_s}|=\sqrt{\lambda_{Qs}^2+\lambda_{Ds}^2} \quad (8)$$

T_e=P($\lambda_{Ds}i_{Ds}$-$\lambda_{Qs}i_{Ds}$)=$\frac{P|\lambda_s|}{2L_dL_q}[2\lambda_f L_q\sin(\theta_s-\theta_r)$-

$|\lambda_s|(L_q-L_d)\sin(2(\theta_s-\theta_r))]$ (9)

where$\lambda_f$is rotor linkage flux and L_d and $L_q$are d-axis and q-axis inductances, respectively. Initial values of D- and Q- axis stator flux components are:

$$\lambda_{Qs}|_{t=0}=\lambda_f\sin\theta_{r0} \quad (10)$$

$$\lambda_{Ds}|_{t=0}=\lambda_f\cos\theta_{r0} \quad (11)$$

where$\theta_{r0}$is initial angle between rotor flux vector and D axis. Block diagram of direct torque control of two-phase induction and synchronous motor is shown in Fig.3 in which at each sampling period, the stator flux modulus and electromagnetic torque are found and a voltage vector which reduces the errors of these parameters is chosen. Electricaltime constant of the rotor of induction motors is large and so the rotor flux doesn't considerably change in a short interval. Thus, a quick torque response can be achieved by rotating the voltage vector in a way that $\theta_s$would increase rapidly. Like induction motor, step change in electromagnetic torque of synchronous motor can be resulted by accelerating stator flux vector leading to change the angle between stator and rotor linkage flux vectors.

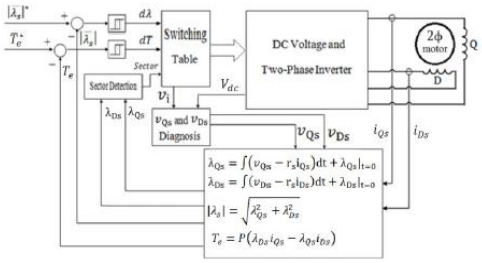

Figure4. Block diagram of direct torque control of two-phase induction motor and synchronous motor

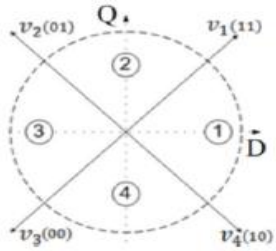

Figure5.Four stator flux sectors generated by voltage vectors of two- leg inverter

TABLE I.DTC SWITCHING TABLE FOR TWO-PHASE MOTORS FED BY TWO-LEG INVERTER

		Flux Sector			
$d\lambda$	dT	1	2	3	4
1	1	v_1	v_2	v_3	v_4
	0	v_4	v_1	v_2	v_3
0	1	v_2	v_3	v_4	v_1
	0	v_3	v_4	v_1	v_2

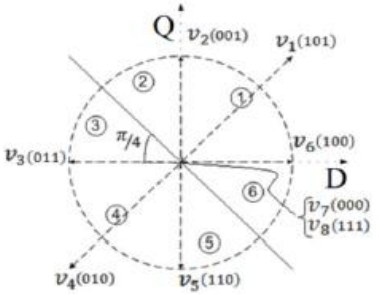

Figure6.Six stator flux sectors generated by voltage vectors of three-leg inverter

TABLE II.DTC SWITCHING TABLE FOR TWO-PHASE MOTORS FED BY THREE–LEG INVERTER

		Flux Sector					
$d\lambda$	dT	1	2	3	4	5	6
1	1	v_2	v_3	v_4	v_5	v_6	v_1
	0	v_7	v_8	v_7	v_8	v_7	v_8
	-1	v_6	v_1	v_2	v_3	v_4	v_5
0	1	v_3	v_4	v_5	v_6	v_1	v_2
	0	v_8	v_7	v_8	v_7	v_8	v_7
	-1	v_5	v_6	v_1	v_2	v_3	v_4

Using DTC method, switching table of two-phasesynchronous motor derive resembles that of induction motor drive, but synchronous motor control method has some constraints:

1. In DTC method, when increasing the electromagnetic torque is desired, the switching table increases the load angle. In "load angle-torque" curve of cylindrical and salient-pole synchronous motors with $(L_d > L_q)$ slope of the curve in stable operating region is always positive, so increase of the load angle leads to increased electromagnetic torque. Therefore, DTC method works properly. When a salient-pole synchronous motor with $(L_d < L_q)$ is being controlled using DTC method, slope of "load angle-torque" curve should be positive to have a perfect torque control.

Regarding, a constraint should be met:

$$|\lambda_s|^* = \frac{L_q}{L_q - L_d}\lambda_f \qquad (12)$$

If is not met, a delay will occur during motorstarting period.

2. Switching table of DTC method is designed to control synchronous motor in stable region of "load angle-torque" curve. If the command torque exceeds the maximum deliverable torque of motor, loss of synchronism occurs. So, the command torque should be less than maximum deliverable torque. The maximum deliverable torque of synchronous motor can be derived as:

$$T_{emax} = \frac{P|\lambda_s|}{2L_dL_q}\left[2\lambda_f L_q \sin(\delta_{max}) - |\lambda_s|(L_q - Ld\sin 2\delta\max)\right) \qquad (13)$$

whereδ_{max} is the maximum load angle that can be expressed as:

$$\delta_{max} = \cos^{-1}\left(\frac{\varepsilon\lambda_f}{4|\lambda_s|} - \frac{\varepsilon}{2|\varepsilon|}\sqrt{\left(\frac{\varepsilon\lambda_f}{2|\lambda_s|}\right)^2 + 2}\right) \qquad (14)$$

Where

$$\varepsilon = \frac{L_q}{L_q - L_d} \qquad (15)$$

3. In the case of synchronous motor control, regarding, precise calculation of stator flux component requires diagnosis of initial position. As position encoder is not utilized in DTC method, the estimation of initial rotor position is formidable. When the initial position estimation is incorrect, the motor initially rotates in wrong direction that restricts usage of synchronous motor DTC drive in some applications .

B. DTC method utilizing two-leg inverter

When the middle point of DC-link power supply isaccessible, DTC of a two-phase motor by a two-leg inverter is possible. Fig.4 shows available voltage vectors generated by two-leg inverter and the way of distinguishing four stator flux sectors using a method similar to presented ones in for three-phase motors. Appropriate switching table for DTC of two-phase induction and synchronous motor fed by two-leg inverter is presented in Table I. When the stator flux vector is near the border of a sector, the component of voltage vector tangent to circular route of the stator flux becomes so small that is not able to reduce torque error and so electromagnetic control method is unable to keep the electromagnetic torque error in allowed band.

C. DTC method utilizing three-leg inverter

Using a three-leg inverter for controlling two-phase motor obviates the need of accessing middle point of DC link voltage. For controlling both flux and electromagnetic torque, six distinct sectors can be specified for the stator flux. The way of doing this and available voltage vectors are shown in Fig. 5. Table II presents the appropriate switching table of two-phase induction and synchronous motor fed by three-leg inverter.

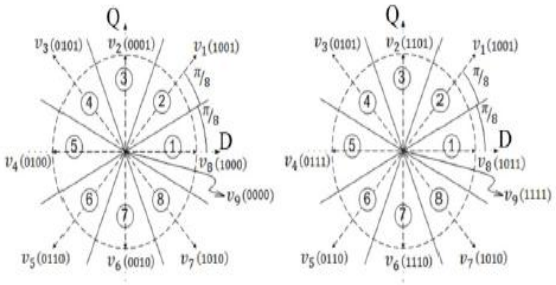

Figure7.Eight stator flux sectors generated by voltage vectors of four-leg inverter using two approaches to generate zero voltage

TABLE III.DTC SWITCHING TABLE FOR TWO-PHASE MOTORS FED BY FOUR LEG INVERTER

		Flux Sector							
dλ	dT	1	2	3	4	5	6	7	8
1	1	v_1	v_2	v_3	v_4	v_5	v_6	v_7	v_8
	0	v_9	v_9	v_9	v_9	v_9	v_9	v_9	v_9
	-1	v_7	v_8	v_1	v_2	v_3	v_4	v_5	v_6
0	1	v_2	v_3	v_4	v_5	v_6	v_7	v_8	v_1
	0	v_9	v_9	v_9	v_9	v_9	v_9	v_9	v_9
	-1	v_6	v_7	v_8	v_1	v_2	v_3	v_4	v_5
-1	1	v_3	v_4	v_5	v_6	v_7	v_8	v_1	v_2
	0	v_9	v_9	v_9	v_9	v_9	v_9	v_9	v_9
	-1	v_5	v_6	v_7	v_8	v_1	v_2	v_3	v_4

TABLE IV.TANGENTIAL COMPONENTS OF VOLTAGE VECTORS GENERATED BY TWO-LEG INVERTER

Tangential component	V_{1t}	V_{2t}
$\frac{\text{Tangential component}}{V_{dc}}$	$\frac{\sqrt{2}}{2}\cos(\theta+\frac{\pi}{4})$	$\frac{\sqrt{2}}{2}\cos(\theta-\frac{\pi}{4})$
Tangential component	V_{3t}	V_{4t}
$\frac{\text{Tangential component}}{V_{dc}}$	$\frac{\sqrt{2}}{2}\cos(\theta-\frac{3\pi}{4})$	$\frac{\sqrt{2}}{2}\cos(\theta-\frac{5\pi}{4})$

In sectors 1 and 4, when the stator flux vector is near the border of the sector, the component of voltage vector tangent to circular route of the stator flux becomes so small that is not able to reduce torque error and so electromagnetic control method is unable to keep the electromagnetic torque error in allowed band. However, because of possessing larger voltage vectors, the ability of three-leg inverter to control electromagnetic torque is more than that of two-leg inverter and its uncontrollable torque region is smaller.

D. DTC method utilizing four-leg inverter

Like three-leg inverters, four-leg inverters also do not need access to middle-point of DC link voltage. For controlling both flux and electromagnetic torque, eight distinct sectors can be specified for the stator flux. The way of doing this and available voltage vectors are shown in Fig.7. Table III presents appropriate switching table for DTC method. Four-leg inverter is able to control electromagnetic torque in a wide range of speed and does not have uncontrollable torque region which is problematic in DTC using aforementioned inverters. As there's always a vector suitable for controlling both flux and torque, these two parameters can be properly controlled by four-leg inverter.

IV. MAXIMUM ROTATING FIELD SPEED OF TWO-PHASE MOTOR IN DTC METHOD

In DTC method, in order to increase the electromagnetic torque, angle of the stator flux vector should increase. Keeping the modulus of the stator flux constant, maximum speed of the rotating field is limited. For obtaining maximum possible speed, it's assumed that mechanical load is light and cannot be equal to command torque even in high speed. In this case, DTC system continually applies voltage vectors which rotate the stator flux in forward direction; electromagnetic torque is not controlled and the rotating field rotates in highest speed possible. For the sake of simplicity, the stator ohmic voltage drop is neglected in the calculations.

A. Maximum speed of rotating field using two-leg inverter

In a two-phase DTC drive using two-leg inverter there are four identical flux sectors, so analysis of the maximum speed in one sector is adequate. It's assumed that stator flux vector is in sector 1, so according to Fig. 4, in order to achieve the maximum rotating speed, one of $v_1$or $v_2$vectorsare chosen to accelerate flux vector based on the output of flux hysteresis controller. The stator flux vector is being rotated by a component of voltage vector tangential to its circular route. The tangential components of

voltage vectors generated by two-leg inverter are presented in table IV. Maximum linear speed of stator flux vector is equal to weighted average of the tangential component ofυ_1 or υ_2.

V_t=$P_{(\upsilon_1)}\upsilon_{1_t}$+$P_{(\upsilon_2)}\upsilon_{2_t}$ (16)

Where $\upsilon_{i\ t}$ is tangential component of $\upsilon_i$and $P_{(\upsilon_i)}$ is the probability of applying voltage vectorυ_i .Probability of applying each voltage vector is proportional to the maximum time interval in which applying that vector maintains the modulus of stator flux in allowed range. Since the amplitude of four voltage vectors generated by two-leg inverter are all the same, the time interval in which a certain voltage vector is applied is proportional to the length of the path of stator flux while the modulus of stator flux is in allowed range. First, it's supposed that the angle between the stator flux vector and D-axis is $\boldsymbol{\theta}$and the modulus of stator flux has reached to its minimum allowed value. As shown in Fig. 7, for increasing both torque and flux, $\upsilon_1$is selected. In Fig.8, $|\bar{\lambda}_s|^*$ is desired modulus of the stator flux and x is the lengthof flux-developing vector. In "OAB" triangle, equation is established:

$x^2+(|\bar{\lambda}_s|^*-\Delta\lambda)^2-2x(|\bar{\lambda}_s|^*-\Delta\lambda)\times\cos(\frac{3\pi}{4}+\boldsymbol{\theta})$

$=(|\bar{\lambda}_s|^*+\Delta\lambda)^2$ (17)

where $\Delta\lambda$ is the width of hysteresis flux controller.

Assuming k=$\frac{\Delta\lambda}{|\bar{\lambda}_s|^*}$and $x'=\frac{x}{|\bar{\lambda}_s|^*}$gives

$x'=\sqrt{4k+(1+k)^2 sin^2\left(\frac{\pi}{4}+\boldsymbol{\theta}\right)-(\mathbf{1}+\boldsymbol{k})\,\mathbf{sin}(\frac{\pi}{4}+\boldsymbol{\theta})}$ **(18)**

"k" has a small value; so regarding McLarenSeries$((\sqrt{k^2+ak+1})_{k\to0}\cong1+\frac{ak}{2})$, results:

$x'=\frac{2k}{\sin(\frac{\pi}{4}+\theta)}$ (19)

where$x'$is normalized length of flux-developing vector.

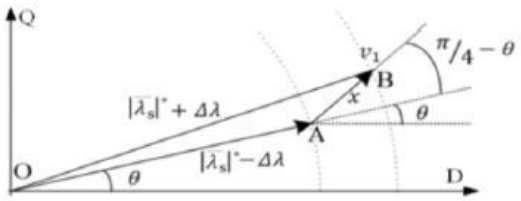

Figure8.Selecting vector $\upsilon_1$in the sector 1 in order to develop stator flux

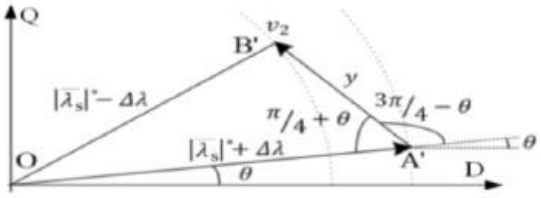

Figure9.Selecting vector $\upsilon_2$in the sector 1 in order to weaken stator flux

TABLE V.TANGENTIAL COMPONENT OF VOLTAGE VECTORS GENERATED BY THREE-LEG INVERTER

Tangential component	V_{1t}	V_{2t}	V_{3t}
Tangential Component / V_{dc}	$\sqrt{2}\cos(\theta+\frac{\pi}{4})$	$\cos(\theta)$	$\cos(\theta-\frac{\pi}{2})$
Tangential component	V_{4t}	V_{5t}	V_{6t}
Tangential Component / V_{dc}	$\sqrt{2}\cos(\theta-\frac{3\pi}{4})$	$\cos(\theta-\pi)$	$\cos(\theta-\frac{3\pi}{2})$

TABLE VI.PROBALITY OF USINGDIFFERENT VOLTAGE VECTORS OF THREE-LEG INVERTER IN SECTORS 1,2,3

	Stator flux sector		
	1	2	3
Normalized length of flux-developing vector	$x'=\frac{2k}{\sin(\theta)}$	$x'=\frac{-2k}{\cos(\theta)}$	$x'=\frac{-2k}{\cos(\theta-\frac{\pi}{4})}$
Normalized length of flux weakening vector	$y'=\frac{2k}{\cos(\theta)}$	$y'=\frac{2k}{\cos(\theta-\frac{\pi}{4})}$	$y'=\frac{-2k}{\cos(\theta-\frac{3\pi}{2})}$
Probability of applying flux-developing vector	$P(\upsilon_2)_1=\frac{\cos(\theta)}{\cos(\theta)+\sin(\theta)}$	$P(\upsilon_3)_2=\frac{\sqrt{2}\cos(\theta-\frac{\pi}{4})}{\sqrt{2}\cos\left(\theta-\frac{\pi}{4}\right)-\cos(\theta)}$	$P(\upsilon_4)_3=\frac{\cos(\theta-\frac{3\pi}{2})}{\cos\left(\theta-\frac{3\pi}{2}\right)+\sqrt{2}\cos(\theta-\frac{\pi}{4})}$
Probability of applying flux weakening vector	$P(\upsilon_3)_1=\frac{\sin(\theta)}{\cos(\theta)+\sin(\theta)}$	$P(\upsilon_4)_2=\frac{-\cos(\theta)}{\sqrt{2}\cos\left(\theta-\frac{\pi}{4}\right)-\cos(\theta)}$	$P(\upsilon_5)_3=\frac{\sqrt{2}\cos(\theta-\frac{\pi}{4})}{\cos\left(\theta-\frac{3\pi}{2}\right)+\sqrt{2}\cos(\theta-\frac{\pi}{4})}$

Now, it's assumed that the modulus of stator flux has reached to its maximum allowed value. In this condition, as shown in Fig. 8, in order to increase electromagnetic torque and reduce the modulus of the stator flux, vector υ_2 is selected. In Fig.8, y is the length of flux weakening vector. Pursuing calculations in "O$A'B'$" triangle analogous to those pursued in "OAB" triangle results:

$y'=\frac{2k}{\cos(\frac{\pi}{4}+\theta)}$ (20)

$y'$is normalized length of flux-weakening vector and is equal to $\frac{y}{|\bar{\lambda}_s|^*}$.So, the probabilities of applying each of these two flux-developing and flux-weakening vectors are as:

$$P_{(v_1)} = \frac{x'}{x'+y'} = \frac{\cos(\frac{\pi}{4}+\theta)}{\sin(\frac{\pi}{4}+\theta)+\cos(\frac{\pi}{4}+\theta)} \quad (21)$$

And

$$P_{(v_2)} = \frac{x'}{x'+y'} = \frac{\sin(\frac{\pi}{4}+\theta)}{\cos(\frac{\pi}{4}+\theta)+\sin(\frac{\pi}{4}+\theta)} \quad (22)$$

Regarding maximum linear speed of stator flux vector can be expressed as:

$$V_t = P_{(v_1)} v_{1_t} + P_{(v_2)} v_{2_t} = \frac{v_{dc}}{2\cos(\theta)} \quad (23)$$

So, the maximum rotational speed of the stator flux Vector throughout a sector is

$$\overline{\omega} = \frac{2}{\pi}\int_{-\frac{\pi}{4}}^{\frac{\pi}{4}} \frac{v_{dc}}{2\cos(\theta)|\overline{\lambda_s}|^*} d\boldsymbol{\theta} \cong 0.56\frac{v_{dc}}{|\overline{\lambda_s}|^*} \quad (24)$$

Regarding the maximum rotating field speed of two-phase motor depends on DC link voltage and the modulus of the stator flux.

B. Maximum speed of rotating field using three-leg inverter

Six sectors of the stator flux can be divided into two identical groups, each including three consecutive sectors. So, sectors 1, 2 and 3 are chosen for calculations. According to Fig.6,tangential components of voltage vectors generated by three-leg inverter are presented in Table V. Like those in two-leg inverter, essential equations for calculating the lengths of flux-developing and flux weakening vectors generated by three-leg inverter and the probability of applying these vectors are derived as functions of the stator flux angle. Table VI presents probability of applying each voltage vector in sectors 1, 2 and 3 when the maximum speed of rotating field is expected$P_{(v_i)_j}$.Presents the probability of using $v_i$in sector j. According to probability functions and tangential components of voltage vectors, maximum angular speed of the stator flux in each sector can be calculated as:

$$\overline{\omega_1} = \frac{2}{|\overline{\lambda_s}|^*}\int_0^{\frac{\pi}{2}} (P_{(v_2)_1} v_{2p} + P_{(v_3)_1} v_{3p}) d\boldsymbol{\theta} \cong$$

$$\mathbf{0.794}\frac{v_{dc}}{|\overline{\lambda_s}|^*} (25) \overline{\omega_2} = \frac{4}{|\overline{\lambda_s}|^*}\int_{\frac{\pi}{2}}^{\frac{3\pi}{4}} (P_{(v_3)_2} v_{3p} +$$

$$P(v4)2v4p)d\boldsymbol{\theta} \cong 1.122vdc\lambda s* \quad (26)$$

$$\overline{\omega_3} = \frac{4}{|\overline{\lambda_s}|^*}\int_{\frac{3\pi}{4}}^{\pi} (P_{(v_4)_3} v_{4p} + P_{(v_5)_3} v_{5p}) d\boldsymbol{\theta} \cong 1.122\frac{v_{dc}}{|\overline{\lambda_s}|^*}$$

(27)

As the stator flux transverses half of the path with average speed $\overline{\omega_1}$and remaining path with average speed $\overline{\omega_2} = \overline{\omega_3}$maximum angular speed of stator flux is $0.93\frac{v_{dc}}{|\overline{\lambda_s}|^*}\frac{rad}{sec}$.

C. Maximum speed of rotating field using four-leg inverter

Like two- and three-leg inverter topologies, for determining maximum rotating field speed of two-phase motors fed by four-leg inverter, it's assumed that voltage vectors which rotate the stator flux vector with highest possible speed and also maintain the modulus of the stator flux in allowed range are used. The values of tangential components of voltage vectors generated by the inverter are required for calculation of maximum speed of rotating field. These values are shown in Table VII based on the voltage vectors illustrated in Fig.6. Eight sectors of the stator flux can be divided into four identical groups each containing 90° of the stator flux angle, so performing calculations in 90° is adequate. Areas 1, 2 that respectively represent $\frac{-\pi}{4} \leq \boldsymbol{\theta} < \mathbf{0}, 0 \leq \boldsymbol{\theta} < \frac{\boldsymbol{\pi}}{\mathbf{4}}$are selected for calculations. Like aforementioned two topologies, the lengths of flux developing and flux-weakening vectors are calculated and then the probability distribution functions are derived as a function of stator flux angle as shown in Table VIII, where$P_{(v_i)_j}$ is the probability of using $v_i$in area j.

TABLE VII.TANGENTIAL COMPONENT OF VOLTAGE VECTORS GENERATED BY FOUR-LEG INVERTER

Tangential component	Tangential Component / V_{dc}	Tangential component	Tangential Component / V_{dc}
V_{1t}	$\sqrt{2}\cos(\theta+\frac{\pi}{4})$	V_{5t}	$\sqrt{2}\cos(\theta-\frac{3\pi}{4})$
V_{2t}	$\cos(\theta)$	V_{6t}	$\cos(\theta-\pi)$
V_{3t}	$\sqrt{2}\cos(\theta-\frac{\pi}{4})$	V_{7t}	$\sqrt{2}\cos(\theta-\frac{5\pi}{4})$
V_{4t}	$\cos(\theta-\frac{\pi}{2})$	V_{8t}	$\cos(\theta-\frac{6\pi}{4})$

TABLE VIII.PROBABILITY OF USING DIFFERENT VOLTAGE VECTORS OF FOUR- LEG INVERTER IN 90°

	Angle of stator flux vector	
	Area1: $\frac{-\pi}{4} \le \theta < 0$	Area2: $0 \le \theta < \frac{\pi}{4}$
Normalized length of flux-developing vector	$x' = \frac{k}{\cos(\theta - \frac{\pi}{4})}$	$x' = \frac{k}{\cos(\theta - \frac{\pi}{2})}$
Normalized length of flux-weakening vector	$y' = \frac{-k}{\cos(\theta - \frac{\pi}{2})}$	$y' = \frac{-k}{\cos(\theta - \frac{3\pi}{4})}$
Normalized length of flux-developing vector	$P(v_1)_1 = \frac{\cos(\theta - \frac{\pi}{2})}{\cos(\theta - \frac{\pi}{2}) - \sqrt{2}\cos(\theta - \frac{\pi}{4})}$	$P(v_2)_2 = \frac{-\sqrt{2}\cos(\theta - \frac{3\pi}{4})}{-\sqrt{2}\cos(\theta - \frac{3\pi}{4}) + \cos(\theta - \frac{\pi}{2})}$
Normalized length of flux-weakening vector	$P(v_2)_1 = \frac{-\sqrt{2}\cos(\theta - \frac{\pi}{4})}{\cos(\theta - \frac{\pi}{2}) - \sqrt{2}\cos(\theta - \frac{\pi}{4})}$	$P(v_3)_2 = \frac{\cos(\theta - \frac{\pi}{2})}{-\sqrt{2}\cos(\theta - \frac{3\pi}{4}) + \cos(\theta - \frac{\pi}{2})}$

According to probability functions and tangentialcomponents of voltage vectors, maximum angular speed of stator flux of direct-torque-controlled-two-phase motor fed by four-leg inverter can be calculated as:

$$\bar{\omega} = \frac{2}{\pi}\int_{\frac{-\pi}{4}}^{\frac{\pi}{4}} \frac{v_{dc}}{|\lambda_s|\cos(\theta)} d\boldsymbol{\theta} \cong \mathbf{1.12}\frac{v_{dc}}{|\boldsymbol{\lambda_s}|} \qquad \textbf{(28)}$$

Thus, keeping the stator flux and DC link voltage Constant, four-leg inverter provides the possibility of operation at higher speeds.

SIMULATION RESULTS:

ROTOR FLUX ANGLE:

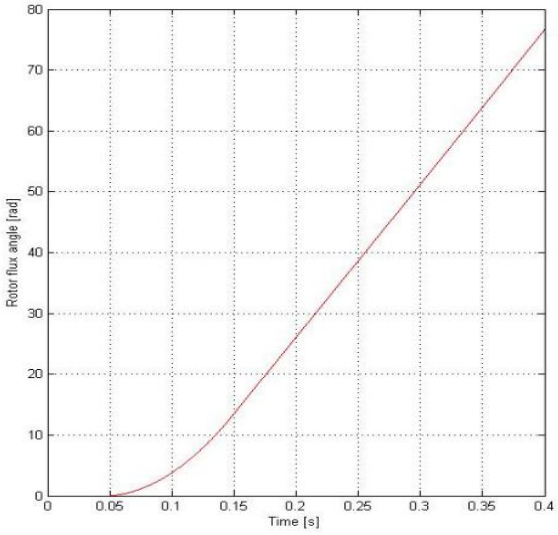

SIMULATION CIRCUIT FOR SSTPI FEDI.M:

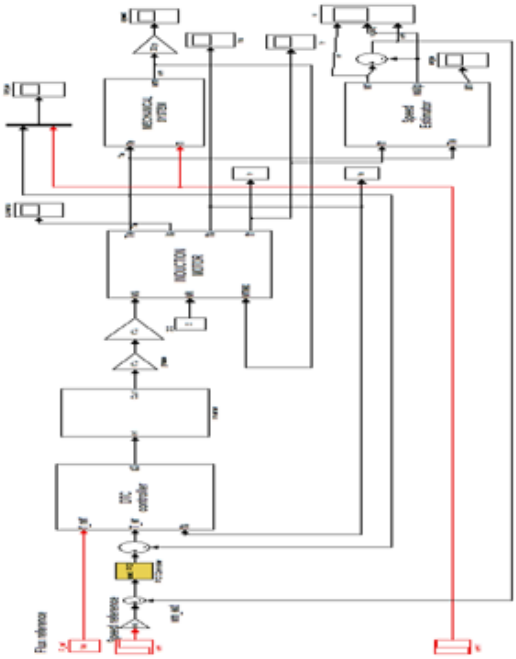

SIMULATION RESULTS FOR SSTPI:

FLUX SPACE VECTOR TRAJECTORY:

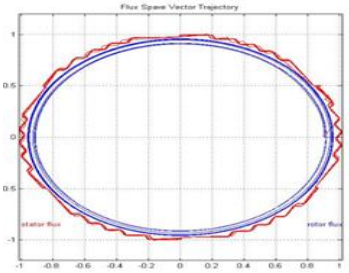

SPEED CURVES:

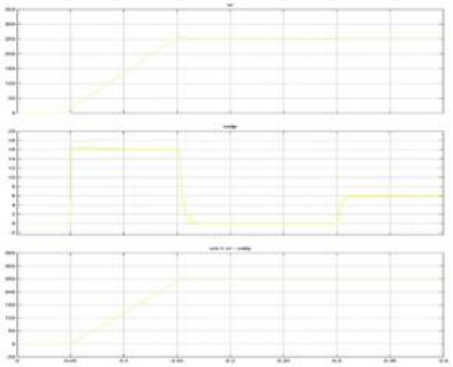

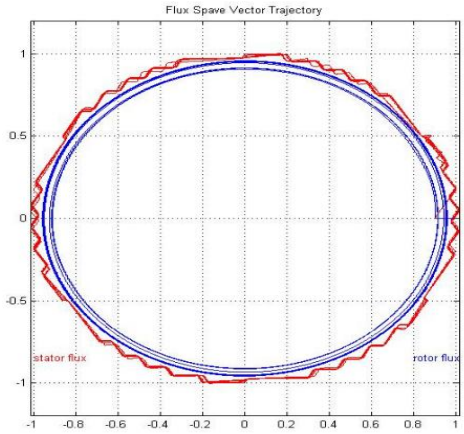

ROTOR FLUX ANGLE:

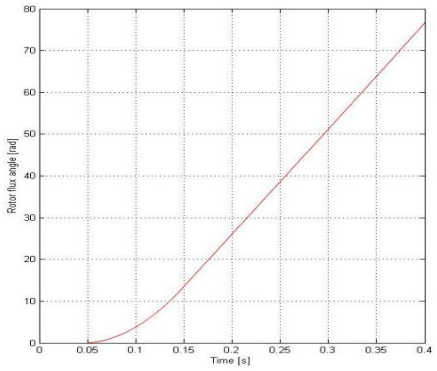

SPEED CURVES:

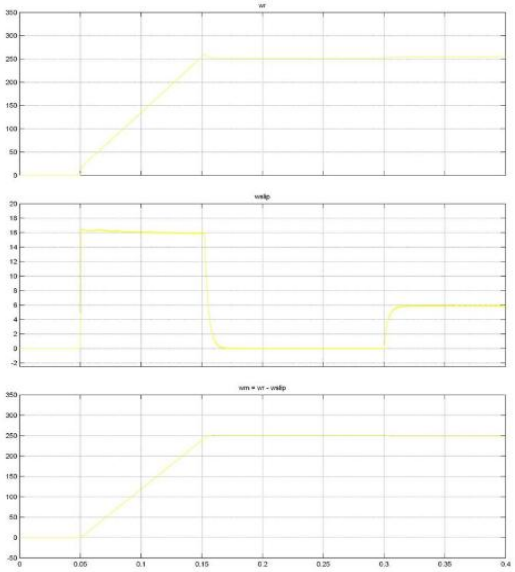

CONCLUSION

The project dealt with a new DTC strategy dedicated to FSTPI fed IM drives. The proposed DTC strategy is based on the emulation of the operation of the conventional SSTPI. This has been achieved thanks to suitable combinations of the four unbalanced voltage vectors intrinsically generated by the FSTPI, leading to the synthesis of the six balanced voltage vectors yielded by the SSTPI. This approach has been adopted in the design of the vector selection table which is simply addressed by hysteresis controllers, considering a subdivision of the *Clarke* plane into six sectors. Simulation-based investigations of the IM steady-state features have revealed the high performance of the introduced DTC strategy. These performances have been the subject of an experimental validation along with a comparison against those yielded by *Takahashi* and the basic DTC strategies dedicated to the SSTPI and to the FSTPI, respectively.

REFERENCES:

[1]. I. Takahashi and T. Noguchi, "A new quick-response and high-efficiency control strategy of an induction motor," *IEEE Trans. Ind. Appl.*, vol. 22, no. 5, pp. 820–827, Sep. 1986.

[2]. Y. Zhang and J. Zhu, "Direct torque control of permanent magnet synchronous motor with reduced torque ripple and commutation frequency," *IEEE Trans. Power Electron.*, vol. 26, no. 1, pp. 235–248, Jan. 2011.

[3]. Y. Zhang, J. Zhu, Z. Zhao, W. Xu, and D. G. Dorrell, "An improved direct torque control for three-level inverter-fed inductionmotorsensorless drive," *IEEE Trans. Power Electron.*, vol. 27, no. 3, pp. 1502–1513, Mar. 2012.

[4]. A. Taheri, A. Rahmati, and S. Kaboli, "Efficiency improvement in DTC of six-phase induction machine by adaptive gradient descent of flux," *IEEE Trans. Power Electron.*, vol. 27, no. 3, pp. 1552–1562, Mar. 2012.

[5]. A. B. Jidin, N. R. B. N. Idris, A. H. B. M. Yatim, M. E. Elbuluk, and T. Sutikno, "A wide-speed high torque capability utilizing overmodulation strategy in DTC of induction machines with constant switching frequency

controller," *IEEE Trans. Power Electron.*, vol. 27, no. 5, pp. 2566–2575, May 2012.

[6]. J. K.Kang, D. W. Chung, and S. K. Sul, "Direct torque control of induction machine with variable amplitude control of flux and torque hysteresis bands," in *Proc. Int. Elect. Mach. Drives Conf.*, Seattle,Washington, May 1999, pp. 640–642.

[7]. K. B. Lee and F. Blaabjerg, "Sensorless DTC-SVM for induction motor driven by a matrix converter using a parameter estimation strategy," *IEEE Trans. Ind. Electron.*, vol. 55, no. 2, pp. 512–521, Feb. 2008.

[8]. Z. Zhifeng, T. Renyuyan, B. Boadong, and X. Dexin, "Novel direct torque control based on space vectormodulationwith adaptive stator flux observer for induction motors," *IEEE Trans. Magn.*, vol. 48, no. 8, pp. 3133–3136, Aug. 2010.

[9]. J. Beerten, J. Verveckken, and J. Driesen, "Predictive direct torque control for flux and torque ripple reduction," *IEEE Trans. Ind. Electron.*, vol. 57, no. 1, pp. 404–412, Jan. 2010.

[10]. T. Geyer, "Computationally efficient model predictive direct torque control," *IEEE Trans. Power Electron.*, vol. 26, no. 10, pp. 2804–2816, Oct. 2011.